

that their criticisms of Shaw's potential for Li do not apply to Na because Shaw modelled both the $l = 0$ and $l = 1$ components here.

Finally, we remark that the dispersion curves for K, calculated with Shaw's potential, agree exceptionally well with the experimental values, at 9°K , of Cowley *et al.* (1966) (see figure 3). The relative errors of the HA potential are the same as for Na and the exchange-correlation corrections have similar significant effects, so we need not discuss these curves further.

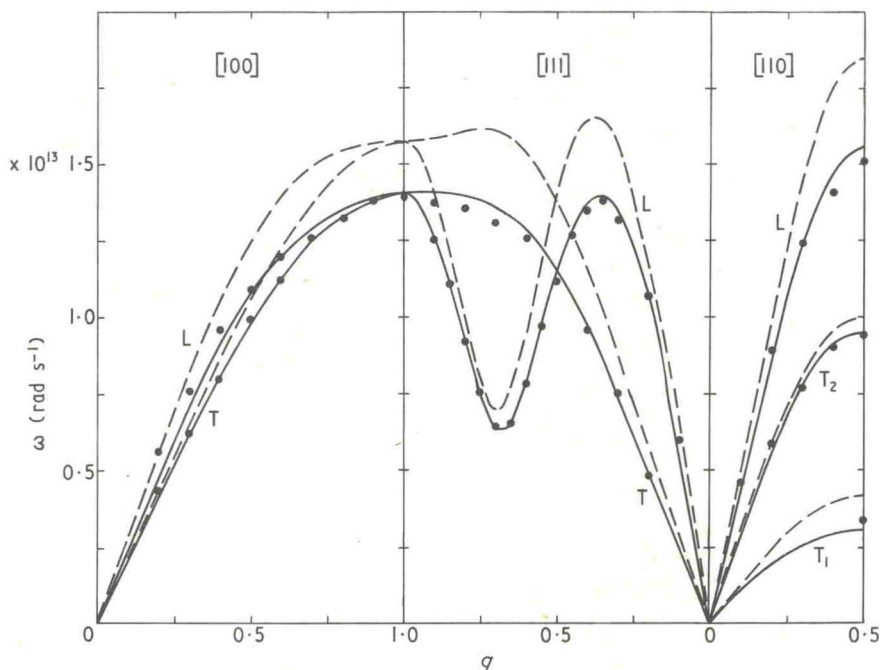


Figure 3. Phonon dispersion curves in K. The full and broken curves are again as in figure 1, and the experimental points are from Cowley *et al.* (1966). Units for the wave vector are as in figure 1.

3.3. Lead

The dispersion curves for Pb, calculated from the local HA potential, are, at best, in only qualitative agreement with experiment. Shaw has not calculated his potential for any element as heavy as Pb.

When the A_l parameters of Animalu and Heine (1965) are used, the lower part of the $[110T_1]$ branch is imaginary, the peaks in the $[100]$ branches are far too small and the phonon frequencies at the zone boundaries are too high, regardless of the dielectric function used. Because of the even greater cancellation of ω_c^2 and ω_E^2 than in Al, the effects of the different forms for $f(q)$ are greater, but the trends are much the same. The dispersion curves calculated with Animalu's semi-non-local potential have more pronounced peaks in the $[100]$ branches but are otherwise unaltered. The nearest neighbour distance in Pb is greater than four core radii, so we again expect the ω_R^2 contributions to be relatively unimportant. Effective mass corrections should be significant, but are unlikely to account for the differences from experiment.

Satisfactory agreement with experiment cannot be obtained even when the A_l parameters are varied arbitrarily, and the pressure derivatives of the elastic constants agree poorly with experiment (Miller and Schuele 1969). This form of potential therefore cannot be used to calculate reliably the phonon dispersion curves in Pb. Vosko *et al.* (1965) and

Harrison (1966) also could only obtain qualitative agreement with experiment by adjusting parameters in their potentials. As they pointed out, spin-orbit effects and effects due to the real Fermi surface and electron wave functions would be important in Pb and would have to be included in any proper theoretical treatment of its phonon dispersion curves.

4. Pressure dependence of maximum phonon frequencies and superconducting transition temperatures

We conclude the study of the model potentials by testing the predicted pressure derivatives of the maximum phonon frequencies for the different branches. They have been used to calculate the pressure derivative of the superconducting transition temperatures, T_c , of Al and Pb, following a method Hodder (1969) has used for Pb. We shall simply outline Hodder's technique here and indicate how we have used it, leaving all detailed discussion of the pressure dependence of T_c , both experimental and theoretical, to a later paper in which results of our detailed study of the electron-phonon interaction and superconductivity will be given (Coulthard, to be submitted for publication).

Hodder's (1969) technique is based on McMillan's (1968) formula for T_c and an approximation of the phonon density of states $F(\omega)$ by a superposition of Lorentzians. Assuming that only the peaks, ω_1^μ , of the Lorentzians move under pressure, he obtained:

$$\frac{d \ln T_c}{dP} = \frac{d \ln \omega_c}{dP} + \frac{1.23}{(\lambda - 0.11)^2} \sum_{\mu=1}^3 \lambda_\mu \left(\frac{d \ln I_\mu}{dP} - 2 \frac{d \ln \omega_1^\mu}{dP} \right) \quad (9)$$

where

$$\lambda = \sum_{\mu=1}^3 \lambda_\mu = \sum_{\mu=1}^3 2 \int_0^\infty \alpha_\mu^2(\omega) F_\mu(\omega) \frac{d\omega}{\omega}$$

$\alpha_\mu^2(\omega) F(\omega)$ is the electron-phonon coupling function (Scalapino *et al.* 1966), ω_c is the maximum phonon frequency, and I_μ depends upon the electron-ion potential:

$$I_\mu = \frac{m^* \Omega}{8\pi^2 k_F} \int_0^{2k_F} \langle (\epsilon_{q\mu} \cdot q)^2 \rangle_{av} v^2(q) q dq.$$

The electron-electron Coulomb pseudopotential has been set equal to 0.10, and the frequency dependence of $\alpha_\mu^2(\omega)$ for each mode μ will be neglected.

In deriving equation (9), Hodder (1969) assumed that $(\omega_2^\mu/\omega_1^\mu)^2 \ll 1$, where ω_2^μ is the half-width of the Lorentzian. Making the same approximation in his equation (5) for λ_μ , we obtain

$$\lambda_\mu \approx \frac{2\alpha_\mu^2}{\omega_1^\mu}$$

while $\alpha_\mu^2 = I_\mu/\omega_1^\mu$ from his equation (8). These equations are equivalent to McMillan's (1968) equation (39), and show that the coupling depends on the model potential mainly through the phonon frequencies. The value of $d \ln T_c/dP$ from (9) is dominated by ω_1^μ and $d \ln \omega_1^\mu/dP$, because we find $d \ln I_\mu/dP$ to be relatively small, so we have an immediate test of our calculated phonon pressure derivatives.

The parameters for the Lorentzian fits to $F(\omega)$ were chosen to reproduce as well as possible the experimental $F(\omega)$ of Stedman *et al.* (1967). For Al, we used $\omega_1^I = 37$, $\omega_2^I = 2$, $\omega_1^T = 21.5$ and $\omega_2^T = 5.3$ meV, and for Pb, 8.5, 0.5, 4.3 and 1.5 respectively; $\omega_3^I = 2\omega_2^I$ throughout. The I_μ integrals have been calculated using the same model potentials as for the phonons; exchange-correlation corrections in the dielectric function are again important, amounting to 20% of I_μ , but affecting the logarithmic derivatives by only about 5%. Our values for the I_μ , $d \ln I_\mu/dP$, α_μ^2 and λ are given in table 6. Likely errors, within the local HA potential approximation, are $\pm 3\%$ for Al and $\pm 10\%$ for Pb. Harrison's (1966) point ion potential yielded values of I_μ which were 10–20% larger, while Shaw's non-local potential predicts values 5–10% smaller than those in the table.